Palestine Journal of Mathematics

Vol 14(Special Issue I)(2025) , 198–211

AN AMPEROMETRIC BIOSENSOR WITH SUBSTRATE INHIBITION KINETICS IN CASE OF ENZYME ALLOSTERY: MATHEMATICAL MODELLING AND ANALYSIS

K. Jegan, M. Mallikarjuna and R. Senthamarai

MSC 2010 Classifications:Primary 34A34; Secondary 35Qxx.

Keywords and phrases: Akbari-Ganji method; amperometric biosensor; allostery enzymes; substrate inhibition; non-Michaelis-Menten kinetics.

The authors would like to thank the reviewers and editor for their constructive comments and valuable suggestions that improved the quality of our paper.

The authors are very thankful for the management of SRM Institute of Science and Technology for their constant support and authors would also thank the Lovely Professional University for giving us the opportunity for publishing our research work through the conference RAFAS-2024.

Corresponding Author: R. Senthamarai

Abstract In this research work, a mathematical model of amperometric biosensor in case of enzyme allostery with substrate inhibition kinetics is analyzed. The model is a non-linear reaction diffusion reaction equations with non-linear terms related to the non-Michaelis-Menten kinetics. The semi-analytical expressions of substrate and product concentrations are obtained using Akbari-Ganji method. The derived results are compared with the numerical simulation using the MATLAB software to obtain the satisfactory of the result. Effects of saturation parameters, Thiele modulus, diffusion constants, kinetic parameters, enzyme layer thickness, bulk substrate concentration and Michaelis-Menten constant on the biosensor current, sensitivity and resistance are analyzed using the derived semi-analytical expressions. The analytical expression of effective membrane thickness of biosensor to obtain the maximum current is also presented. The obtained results are very useful in improving the characteristics of biosensor to achieve a better amperometric response.

1 Introduction

Biosensor has a crucial role in biological sciences, which is an element with a transducer to detect and measure specific biological substances, converting biological responses into measurable signals. Amperometric biosensors detect alterations in the current in its output at the working electrode caused by the direct oxidation or reduction of a biochemical reaction [1, 2, 3]. Extensively utilized due to their efficacy and heightened sensitivity, these biosensors are applied in diverse fields such as food analysis, environmental monitoring, drug analysis, and clinical diagnostics. Amperometric methodologies exhibit a linear correlation with the concentration of the analyte, delivering a response of the current that escalates proportionally as the concentration increases within a standard dynamic range. The accuracy and dependability of these methods for determining analyte concentration are guaranteed by careful experimental condition management and calibration [4, 5, 6].

Enzymes in biosensors are often inhibited by their substrates [1]. Theoretical models are widely used to study and optimize biosensor analytical characteristics. Practical biosensors feature a multilayer enzyme membrane, while exploratory monolayer membrane-containing biosensors are employed for studying biochemical behavior. Manimozhi et al. [7] analyzed a mathematical model of an amperometric biosensor considering the mixed enzyme kinetics with substrate inhibition. The model is a steady-state non-linear reaction-diffusion equation. They have provided an approximate analytical expression for the substrate concentration by utilizing the

Homotopy perturbation method (HPM) and compared with the numerical results. Swaminathan et al. [8] provided semi-analytical expressions for both the substrate and product concentrations of the amperometric biosensor with substrate inhibition by utilizing the Adomian decomposition method (ADM) and the new Homotopy perturbation method (NHPM). Agarwal [9] also employs the HPM for solving the non-linear differential equation governing the flow of a non-Newtonian visco-inelastic fluid between two disks.

To streamline the characteristics of biosensors, a mathematical model based on the substrate and product inhibition is also created. Šimelevičius and Baronas [3] proposed a mathematical model of the amperometric biosensor considering both the substrate and product inhibition with external and internal mass transfers. Recently, Mallikarjuna and Senthamarai [10] analyzed this model and provided approximated analytical results for the substrate and product concentrations by utilizing TSM and ADM and compared with the numerical results. They have also analyzed the current response, sensitivity, and resistance of the biosensor. To the best of our knowledge, there is no existing approximate analytical expression for the mathematical model of the amperometric biosensor with the enzyme allostery. A comprehensive understanding of the kinetic intricacies associated with biosensors is imperative for enhancing their efficiency. This understanding enables the optimization of biosensor configurations, leading to a more accurate prediction of electrode responses. In a recent study, Rasheed and Balasim [11] investigated the blow-up behavior of the reaction-diffusion equation subject to Dirichlet boundary conditions. Their approach involved employing a finite difference scheme to solve the semi-linear heat equation.

This study presents the biosensor model comprising the kinetics of the allostery enzymes. It is observed that variations in the physical and kinetic parameters present in the system allowed the biosensor's peak response to be reached throughout a wide range of substrate and product concentrations. An analytical solution to the system is thought to be more beneficial and convincing than numerical simulations due to its conciseness. This is due to the fact that it facilitates data management and allows for the optimization of delicate parameters in a variety of applications. In this article, the approximate analytical expressions of the steady-state concentrations of substrate and product are analyzed for all values of the kinetic and reaction diffusion parameters that occur in the system, together with the biosensor current response, sensitivity, resistance and effective membrane thickness.

The research article is articulated as follows: Section 2 represents the mathematical formulation of the amperometric biosensor with the substrate inhibition in enzyme allostery. In Section 3, the approximate analytical expressions for the substrate and product concentrations, sensitivity, and resistance are provided. In Section 4, the analytical results are validated by comparing with the obtained numerical simulation. Section 5 provides the major findings of the research work. The conclusion is provided in Section 6 followed by the appendices.

2 Mathematical formulation

The enzyme reaction equation operates a biosensor in generally defined as follows [3],

$$E + S[k_{-1}]k_1 ES \xrightarrow{k_2} E + P \tag{2.1}$$

In the context of the reaction, where E represents an enzyme and S denotes a substrate, the formation of the enzyme-substrate complex (ES) precedes the generation of the product (P). The kinetic parameters k_1 and k_{-1} govern the formation and dissociation of the enzyme-substrate complex, while k_2 represents the rate constant for the conversion of the enzyme-substrate complex to the product.

In this article, a non-Michaelis-Menten kinetics of homotropic allosteric enzyme activity is considered (allostery modulator is substrate itself). Where the reversible interaction of an allosteric modulator (A) with the enzyme (E) at a site distinct from the active site results in the generation of an allosterically modulated enzyme (AE).

$$A + E[k_{-a}]k_a AE \tag{2.2}$$

The kinetics of this interaction, specifically the association rate constant k_a and the dissociation rate constant k_{-a}, were systematically characterized to illustrate the dynamics of the allosteric

modulation process. The regulatory effects of allosteric modulators on enzyme activity are explained, offering important insights into the molecular mechanisms underlying them.

$$S + AE \xrightarrow{k_2} EAS \tag{2.3}$$

The allostery enzyme-substrate complex denoted as EAS, emerges as the substrate binds with the allosteric enzyme EA, where k_2 characterizes the rate constant of the reaction.

$$EAS \xrightarrow{k_5} E + P \tag{2.4}$$

In the catalytic cycle, the final step involves the liberation of the product P, where k_5 signifies the rate constant governing this release process. This pivotal stage denotes the culmination of the enzymatic reaction, marking the completion of the catalytic cycle. The mathematical model considering the above allosteric activity is developed as [5]:

$$D_s \frac{d^2 s(x)}{dx^2} = v(s,p) \tag{2.5}$$

$$D_p \frac{d^2 p(x)}{dx^2} = -v(s,p), \qquad 0 \le x \le p \tag{2.6}$$

where,

$$v(s,p) = \frac{E_0 s(k_2 k_a + k_5 s)}{k_m k_a + k_a s + s^2} \tag{2.7}$$

with the following the boundary conditions:
when $x = 0$

$$s'(x) = 0,\ p(x) = 0 \tag{2.8}$$

when $x = d$

$$s(x) = s_0,\ p(x) = 0 \tag{2.9}$$

The model presupposes that the substrate doesn't experience any reactions involving electrons and that the result displays electroactivity. The following is the expression for the biosensor's current density:

$$\Psi = n_e F D_p \left.\frac{dp}{dx}\right|_{x=0} \tag{2.10}$$

By using the dimensionless parameters indicated below in, Eqs. (2.5) and (2.6) are rendered dimensionless:

$$S(\chi) = \frac{s(x)}{s_0}, \quad P(x) = \frac{p(x)}{s_0}, \quad \chi = \frac{x}{d}, \quad \phi_1^2 = \frac{d^2 E_0 k_2}{D_s k_m} \tag{2.11}$$

$$\phi_2^2 = \frac{d^2 E_0 k_2}{D_p k_m}, \quad \alpha = \frac{s_0 k_5}{k_2 k_a}, \quad \beta = \frac{s_0}{k_m}, \quad \gamma = \frac{s_0^2}{k_m k_a}, \ \eta = \frac{k_m}{s_0} \tag{2.12}$$

The concentrations of substrate and product is denoted by S and P, respectively, are dimensionless, and the reaction diffusion parameters, or Thiele modules, are indicated by the values ϕ_1^2 and ϕ_2^2. χ represents the dimensionless distance, while the saturation parameters are denoted by α, β, and γ. The following describes a system of dimensionless form that represents the non-linear reaction diffusion Eqs. (2.5) and (2.6).

$$\frac{d^2 S(\chi)}{d\chi^2} = \phi_1^2 \frac{S + \alpha S^2}{1 + \beta S + \gamma S^2} \tag{2.13}$$

$$\frac{d^2 P(\chi)}{d\chi^2} = -\phi_2^2 \frac{S + \alpha S^2}{1 + \beta S + \gamma S^2} \tag{2.14}$$

with the dimensionless boundary conditions are as follow:
when $\chi = 0$

$$S'(0) = 0,\ P(0) = 0 \tag{2.15}$$

when $\chi = 1$

$$S(1) = 1,\ P(1) = 0 \tag{2.16}$$

and the dimensionless current is as follows:

$$\Psi = \frac{I}{n_e F D_p} \frac{d}{s_0} = \left.\frac{dP}{d\chi}\right|_{x=0} \tag{2.17}$$

3 Substrate and product concentrations

In addressing the challenges associated with obtaining analytical solutions for nonlinear systems, researchers go with approximate analytical methods over numerical ones due to the latter's notable drawbacks, such as issues related to numerical stability and the intricate task of parameter adjustment to align with the numerical data. Analytical solutions are favored for their ability to offer deeper insights into the impact of model parameters. Over the past four decades, numerous reliable semi-analytical methods have emerged, proving successful in approximate nonlinear models across various scientific domains. Notable methods include HPM [13, 14, 15, 16, 17], Variational Iteration Method [18, 19, 20], Homotopy Analysis Method [21, 22, 23], TSM [24, 25, 26], ADM [12, 27] and [28, 29, 30] and AGM [31, 32]. In this article, we applied the AGM for desiring the expressions of substrate and product.

3.1 Approximate analytical expressions using the Akbari-Ganji mathod(AGM)

The solution of substrate and product concentrations by Akbari-Ganji method is obtained as (see appendix B):

$$S(\chi) = \frac{\cosh(m\chi)}{\cosh(m)} \tag{3.1}$$

where

$$m = \sqrt{\frac{\phi_1^2(1+\alpha)}{1+\beta+\gamma}} \tag{3.2}$$

Eqn. (3.2) is obtained by using Eqn. (B3) with $\cosh m \approx 1$ (since for smaller value of m, $\cosh m \approx 1$)
The relation between S(χ) and P(χ) (see appendix A) is as follows:

$$P(\chi) = \frac{\phi_2^2}{\phi_1^2}\left[(1-\operatorname{sech}(m))\chi + \operatorname{sech}(m) - \cosh(m\chi)\operatorname{sech}(m)\right] \tag{3.3}$$

From Eqn. (3.4), we have derived the dimensionless current as follows:

$$\Psi = \frac{I}{n_e F D_p}\left[\frac{d}{s_0}\right] = \frac{\phi_2^2}{\phi_1^2}\left(1 - \frac{1}{\cosh(m)}\right) \tag{3.4}$$

and the current in its dimension form is

$$\Psi = \frac{n_e F s_0 D_s D_p}{d}(1-\cosh(\kappa)) \tag{3.5}$$

where

$$\kappa = \sqrt{\frac{d^2 E_0(k_2 k_a + s_0 k_5)}{D_s(k_m k_a + s_0 k_a + s_0^2)}} \tag{3.6}$$

3.2 Biosensor Sensitivity

One of the most pivotal attribute of the amperometric biosensor is its sensitivity. It is defined as the change of biosensor maximal current rate with respect to the bulk substrate concentration s_0 in the enzyme membrane layer. The analytical expression of the biosensor sensitivity can be obtained from the current equation Eq. (3.5) as follows:

$$B_S = \frac{\partial \Psi(s_0)}{\partial s_0}\frac{s_0}{\Psi(s_0)} = \frac{(-k_2 k_a^2 + (-2k_2 s_0 + k_5 k_m)k_a - k_5 s_0^2)d\; k_2 \sinh(\kappa) d^2}{2\kappa D_s \cosh(\kappa)(cosh(\kappa)-1)((k_m+s_0)k_a + s_0^2)^2} \tag{3.7}$$

3.3 Biosensor resistance

To understand the response of membrane-based biosensors, one must grasp the significance of fluctuations in membrane thickness. In order to evaluate this effect, the gradient of the steady-state biosensor current with respect to the thickness of the enzyme layer d is used to construct the biosensor normalized dimensionless resistance B_R. This idea is especially important for predicting the impact of changes in membrane thickness on the biosensor response.The constant-state biosensor current, or $I(d)$, at the enzyme layer thickness of d is computed here.

$$B_R = \frac{\partial \Psi}{\partial\, d}\frac{d}{\Psi(d)} = -\left(\frac{s_0 E_0(k_2 k_a^2 + (2k_2 s_0 - k_5 k_m)k_a + k_5 s_0^2)\sinh(\kappa)}{2\kappa D_s \cosh(\kappa)(\cosh(\kappa)-1)((k_m+s_0)k_a + s_0^2)}\right) \tag{3.8}$$

4 Validation of analytical results

Using AGM the approximate analytical expressions of non-linear governing equations Eqs. (2.13) and (2.14) with boundary conditions Eqs. (2.15) and (2.16) are obtained. The numerical simulations are done using MATLAB software ODE45 and are compared with the AGM solutions Eqs. (3.1) - (3.3). Fig. 1 and Fig. 2 and Table. 1 and Table. 2 represent the comparison between numerical and AGM solutions. From the error percentage obtained in the table, it is seen that the maximum error between the numerical and AGM for substrate is 0.05% and for the product is 0.69%.

5 Result and Discussion

Figs. 1(a) - 1(c) represent the effect of various parameters on the dimensionless substrate concentration $S(\chi)$. From these figures, the concentration of substrate is an increasing function as it increases as the dimensionless distance χ increases. Also, it increases as the values of the saturation parameter β increase (Fig. 1(a)) but it is inversely proportional for the saturation parameter α (Fig. 1(b)) and the Thiele modulus ϕ_1^2 (Fig. 1(c)) as the values increase, the concentration decreases, and it attains its uniform state when $\beta \geq 100,\ \alpha \leq 0.1,\ \phi_1^2 \leq 0.1$.

Figs. 2(a) - 2(c) represent the effect of various parameters on the dimensionless product concentration $P(\chi)$. From the figures, it is seen that the concentration of product is increasing with the increment in saturation parameter α (Fig. 2(a)) and the Thiele modulus ϕ_2^2 (Fig. 2(c)), and whereas it is an inverse function for the saturation parameter γ (Fig. 2(b)). The concentration becomes uniform when the parameter values are $\phi_2^2 \leq 0.1,\ \alpha \leq 0.1,\ \gamma \geq 100$. It is observed that the product increases gradually from $\chi = 0$ and then attains its maximum at $\chi = 0.5$ and then gradually decreases to 0 at $\chi = 1$.

Another most critical parameter is the biosensor current related to the electroactive material flux. Eq. (3.4) represents the simple closed-form semi-analytical expression of the steady-state current. Fig. 3 represents the current response for various values of the saturation parameters $\alpha,\ \beta,\ \gamma$. From these figures, it is noted that the Thiele modulus ϕ_2^2 has the major impact on the biosensor current, as its value increases current also increases.

5.1 Sensitivity

Sensitivity is another important characteristic that shows the detection capability of the amperometric biosensor to the changes in the biological substance. Figs. 4(a) - 4(d) displays the sensitivity B_S plots of the biosensor with the enzyme allostery versus the bulk substrate concentrations for different parameter values of diffusion and kinetic parameters. It is evident from the figures that sensitivity increases when there is an increase in parameters. When the bulk substrate concentration s_0 is 10^2, the sensitivity attains its lowest value zero and then progressively rises to its maximum $B_S = 1$ when $s_0 \approx 10^6$.

From Fig. 4, it is seen that the increase in values of the membrane thickness d (Fig. 4(a)), total enzyme concentration E_0 (Fig. 4(c)), and kinetic parameter k_5 (Fig. 4(d)) shifts the sensitivity curve to the right direction, whereas the increase in the diffusion parameters D_s, D_p (Fig. 4(b)) shifts the sensitivity curve to the left direction. The kinetic parameters $k_m,\ k_2,\ k_a$ do not have a considerable impact on the biosensor sensitivity.

Table 1. Comparison of numerical solution versus semi-analytical expression Eq. (3.1) with the parameters $\phi_1^2 = 0.4$, $\phi_2^2 = 0.5$, $\alpha = 2$, $\beta = 5$ when $\gamma = 2,\ 10$ and 100.

	$\gamma = 2$			$\gamma = 10$			$\gamma = 100$		
χ	Numerical	AGM	Error%	Numerical	AGM	Error%	Numerical	AGM	Error%
0.0	0.97110	0.97187	0.07833	0.98551	0.98579	0.02903	0.99779	0.99779	0.00004
0.2	0.97472	0.97536	0.06624	0.98732	0.98757	0.02487	0.99806	0.99806	0.00016
0.4	0.98074	0.98120	0.04736	0.99034	0.99053	0.01834	0.99852	0.99851	0.00034
0.6	0.98916	0.98940	0.02354	0.99457	0.99467	0.01006	0.99915	0.99915	0.00057
0.8	0.99999	0.99997	0.00271	1.00001	1.00002	0.00086	0.99997	0.99996	0.00083
1	0.96990	0.97070	0.08248	0.98490	0.98520	0.03046	0.99770	0.99770	0.00000
Average error %			0.04920			0.01893			0.00032

Table 2. Comparison of numerical solution versus semi-analytical expression Eq.(3.3) with the parameters $\phi_1^2 = 0.4$, $\phi_2^2 = 0.5$, $\alpha = 2$, $\beta = 5$ and when $\gamma = 2,\ 10$ and 100.

	$\gamma = 2$			$\gamma = 10$			$\gamma = 100$		
χ	Numerical	AGM	Error%	Numerical	AGM	Error%	Numerical	AGM	Error%
0	0.00000	0.00000	0.00000	0.00000	0.00000	0.00000	0.00000	0.00000	0.00000
0.2	0.00752	0.00744	1.03163	0.00377	0.00373	1.21205	0.00057	0.00056	0.35347
0.4	0.01128	0.01119	0.84541	0.00566	0.00560	1.07394	0.00085	0.00085	0.33706
0.6	0.01128	0.01121	0.60698	0.00565	0.00560	0.89082	0.00085	0.00085	0.32172
0.8	0.00752	0.00749	0.29553	0.00376	0.00374	0.62115	0.00057	0.00057	0.32819
1	0.00000	0.00000	0.00000	0.00000	0.00000	0.00000	0.00000	0.00000	0.00000
Average error%			0.69489			0.63299			0.22341

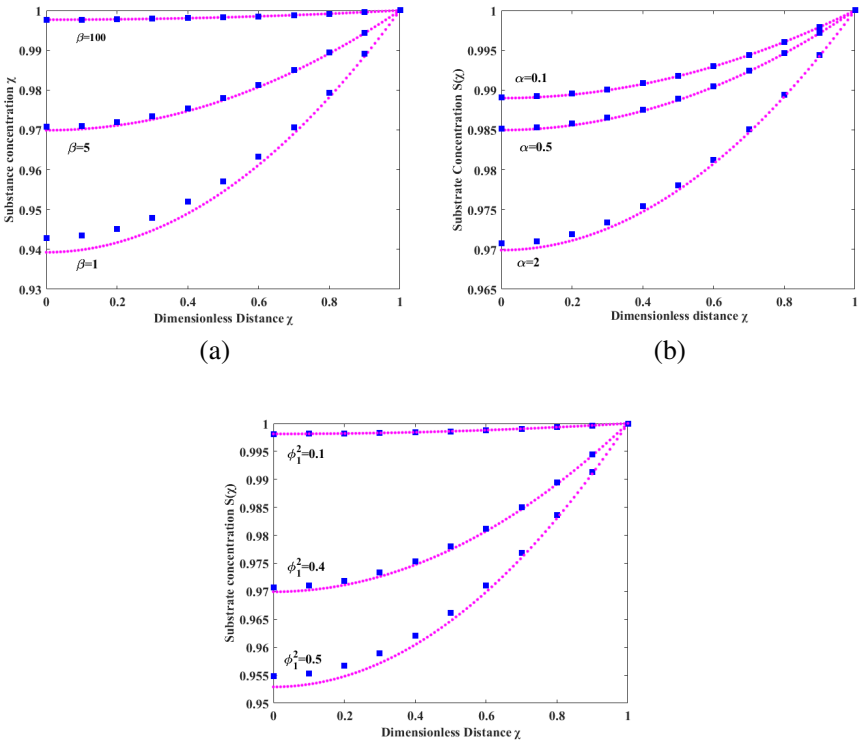

Figure 1. $S(\chi)$ vs χ with the parameters $\phi_1^2 = 0.4$, $\phi_2^2 = 0.5$, $\alpha = 2$, $\gamma = 2$ and $\beta = 5$, when the saturation parameters are (1(a)) $\beta = 1$, $\beta = 5$ and $\beta = 100$ and for (1(b)) $\alpha = 0.1$, $\alpha = 0.5$ and $\alpha = 2$ and (1(c)) Thiele modules is as $\phi_1^2 = 0.1$, $\phi_1^2 = 0.4$ and $\phi_1^2 = 1$ where '$\cdots$' represent the numerical solution and ■■■ represent the AGM solution.

5.2 Resistance

The resistance B_R versus the membrane thickness d for different parameters is given in Fig. 5 and Fig. 6. It shows that the normalized resistance curves follow a recurring pattern. According to these findings, the resistance of the biosensor is inversely proportional to an increase in membrane thickness d started; otherwise, the maximal and minimal resistance of the biosensor are directly proportional to the Thiele modules. The range of B_R is -1 to 1, and there is a non-monotonic relationship between the biosensor current Ψ and the enzyme layer thickness d. The thickness d has more impact to give a high response in the biosensor when B_R is -1 to 1.

It is seen that the increase in values of diffusion parameters $D_s,\ D_p$ and the bulk substrate concentration s_0 shift the resistance curve in the right direction. Whereas total enzyme concentration E_0, kinetic parameters $k_s,\ k_5,\ k_2$ shift resistance curve in opposite direction. The Michaelis-Menten constant k_m doesn't have a significant effect on the resistance of the biosensor. Notably, biosensor resistance behavior is significantly altered when the biosensor moves from a kinetics-limited state to a diffusion-controlled one. This change is especially noticeable at moderate substrate concentrations.

5.3 Effective membrane thickness

By making use of Eq. (3.5), the approximate analytical values of the membrane thickness d can be determined at when the steady-state current reaches its maximum for the given specific parameters: $E_0,\ k_m,\ k_a,\ k_2, k_5, s_0, D_s, D_p$. Eq. (3.5) can be written as

$$\frac{\Psi(d)}{n_e F} = \frac{s_0 D_s D_p}{d}(1 - \operatorname{sech}(\kappa)) \tag{5.1}$$

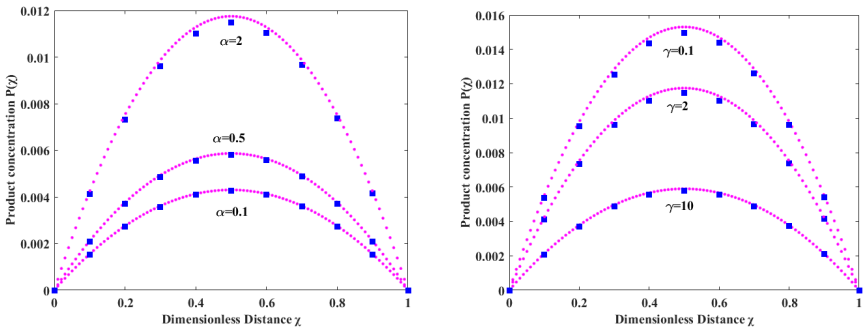

(a) (b)

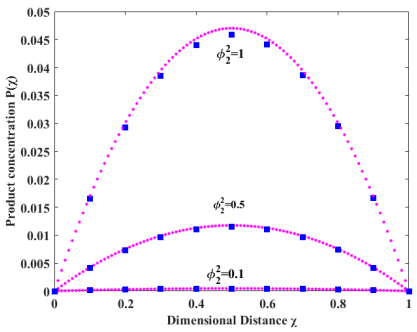

(c)

Figure 2. $S(\chi)$ vs χ with the parameters $\phi_1^2 = 0.4$, $\phi_2^2 = 0.5$, $\alpha = 2$, $\gamma = 2$ and $\beta = 5$, when the saturation parameters are (2(a)) $\beta = 1$, $\beta = 5$ and $\beta = 100$, for (2(b)) $\alpha = 0.1$, $\alpha = 0.5$ and $\alpha = 2$ and (2(c)) Thiele modules is as $\phi_2^2 = 0.1$, $\phi_2^2 = 0.4$ and $\phi_2^2 = 1$ where '$\cdots$' represent the numerical solution and ■■■ represent the AGM solution.

by differentiating Eq.(5.1) with respect to d we obtain the following expression

$$\frac{\partial \Psi(d)}{\partial d} = \frac{n_e F D_s D_p}{d} \frac{-\cosh^2(\kappa) + \kappa \sinh(\kappa) + \cosh(\kappa)}{\cosh^2(\kappa)} \tag{5.2}$$

and we are getting the thickness of the current attains zero

$$-\cosh^2(\kappa) + \cosh(\kappa) + \kappa \ \sinh(\kappa) = 0 \tag{5.3}$$

Numerical solution of Eq. (5.3) yield a unique value of $\kappa_{max} \approx 1.5055$. Consequently, leading to the membrane thickness d at which the maximum current Ψ is attained, where

$$d_{max} = \kappa_{max} \sqrt{\frac{D_s(k_m k_a + s_0 k_a + s_0^2)}{d^2 E_0(k_2 k_a + s_0 k_5)}} = 5.8572 \mu m \tag{5.4}$$

at $E_0 = 50 \mu m/s,\ k_m = 10 \mu m,\ k_a = 10 \mu m,\ k_2 = 100 \mu m,\ k_5 = 100 \mu m,\ s_0 = 100 \mu m,\ D_s = D_p = 300 \mu m^2/s$.

6 Conclusion

A mathematical model of amperometric biosensors with enzyme allostery has been successfully investigated. Using the AGM for substrate and product concentrations. In order to achieve a satisfying outcome, the system's numerical solution is also generated using the MATLAB software and compared with our approximate analytical expression for all parameters and found the obtained results are satisfactory.

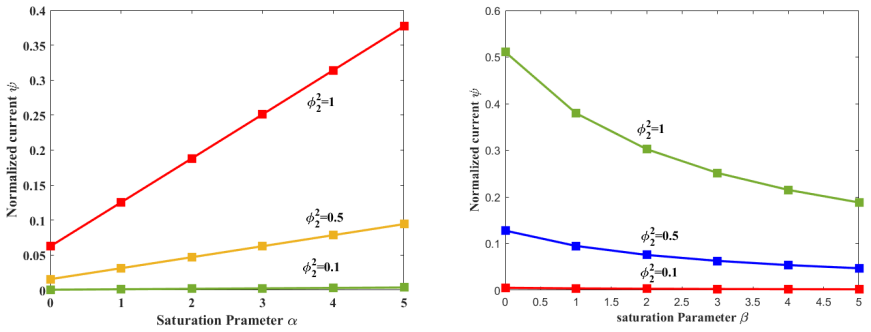

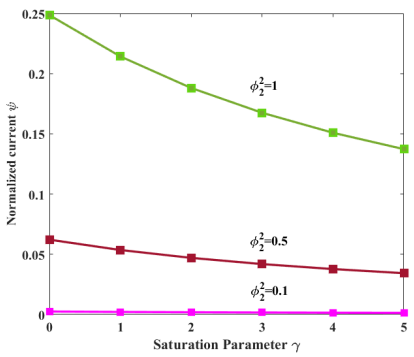

Figure 3. Normalized current ψ saturation parameters (3(a)) α when $\beta = 5$, $\gamma = 2$; (3(b)) β when $\alpha = 2$, $\gamma = 2$ and (3(c)) γ when $\alpha = 2$, $\beta = 5$ for different values is ϕ_2^2 , where'$\cdots$' represent the numerical solution and ■■■ represent the AGM solution.

Additionally, the effective thickness of the enzyme membrane layer is examined, and the semi-analytical expressions for biosensor current, sensitivity, and resistance are also developed. The biosensor current is directly impacted by the diffusion parameter ϕ_2^2; as it rises, so does the biosensor current.

At membrane thickness $d_{max} = \kappa_{max}\sqrt{D_s(k_m k_a + s_0 k_a + s_0^2)/d^2 E_0(k_2 k_a + s_0 k_5)}$, the maximum current is attained. The experimental scientists can get the given theoretical results useful in improving their comprehension and optimizing the biosensor to achieve a better amperometric response.

Appendix A: Relation between substrate and product Concentration

Now we add the Eq.(2.13) and Eq.(2.14)

$$\frac{d^2S(\chi)}{d\chi^2} + \frac{d^2P(\chi)}{d\chi^2} = 0 \tag{.1}$$

let integrate twice Eq.(.1),we have

$$\frac{S(\chi)}{\phi_1^2} + \frac{P(\chi)}{\phi_2^2} = D_1\chi + D_2 \tag{.2}$$

$$P(\chi) = \phi_2^2\left[D_1\chi + D_2 - \frac{S(\chi)}{\phi_1^2}\right] \tag{.3}$$

The substrate solution at $\chi = 0$ from Eq. (2.15), we have:

$$0 = \phi_2^2\left[D_2 - \frac{S(0))}{\phi_1^2}\right] \tag{.4}$$

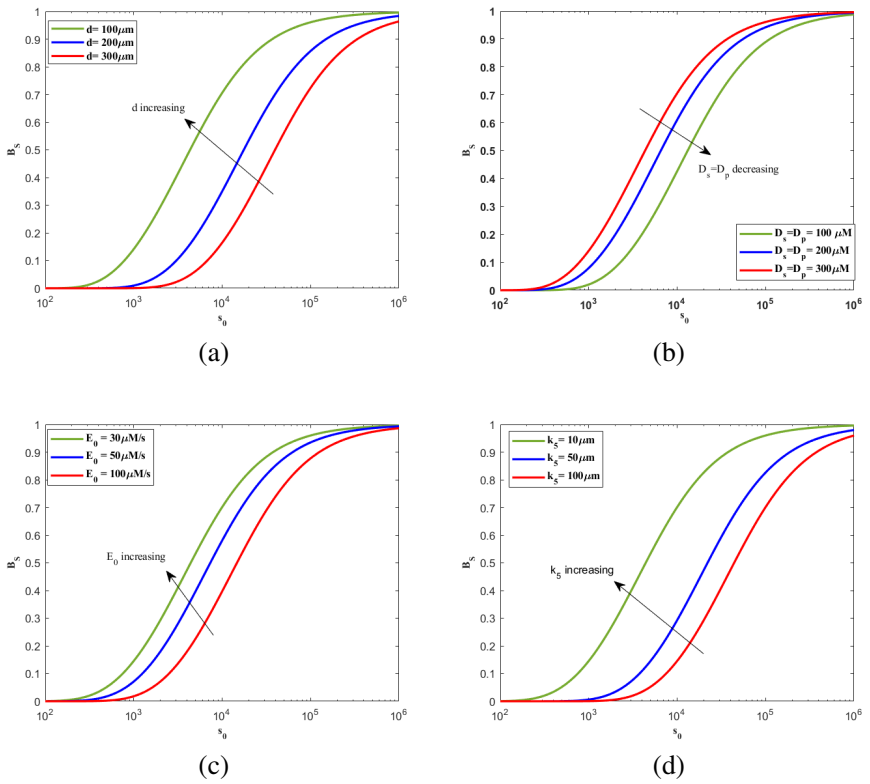

Figure 4. Sensitivity Eq.(3.7) vs bulk substrate concentration s_0 with the parameters $D_s = D_p = 300\mu m^2/s$, $d = 100\mu m^2/s$, $k_m = 10\mu m$, $k_2 = 10\mu m$, $E_0 = 30\mu m/s$, $k_a = 10\mu m/s$, $k_5 = 10\mu m/s$ and for different parameter values (4(a)) enzyme membrane layer thickness d (4(b)) diffusion coefficients of substrate and product D_S, D_P (4(c)) total enzyme concentrations E_0 (4(d)) kinetic parameter k_5.

$$D_2 = \frac{S(0)}{\phi_1^2} \tag{.5}$$

Substitute the Eq. (.5) in Eq. (.3), we get:

$$P(\chi) = \phi_2^2 \left[D_1 \chi + \frac{S(0)}{\phi_1^2} - \frac{S(\chi)}{\phi_1^2} \right] \tag{.6}$$

apply the Eq. (2.16) in Eq. (.6), we get:

$$0 = \phi_2^2 \left[D_1 + \frac{S(0)}{\phi_1^2} - \frac{1}{\phi_1^2} \right] \tag{.7}$$

$$D_1 = \frac{1 - S(0)}{\phi_1^2} \tag{.8}$$

substitute Eq. (.8) and Eq. (.5) in Eq. (.6) we obtain:

$$P(\chi) = \phi_2^2 \left[\left(\frac{1 - S(0)}{\phi_1^2} \right) \chi + \frac{S(0)}{\phi_1^2} - \frac{S(\chi)}{\phi_1^2} \right] \tag{.9}$$

Appendix B: Analytical expression of substrate and product concentrations by AGM

Let us assume that the substrate concentration as:

$$S(\chi) = A \cosh(m\chi) + B \sinh(m\chi) \tag{B1}$$

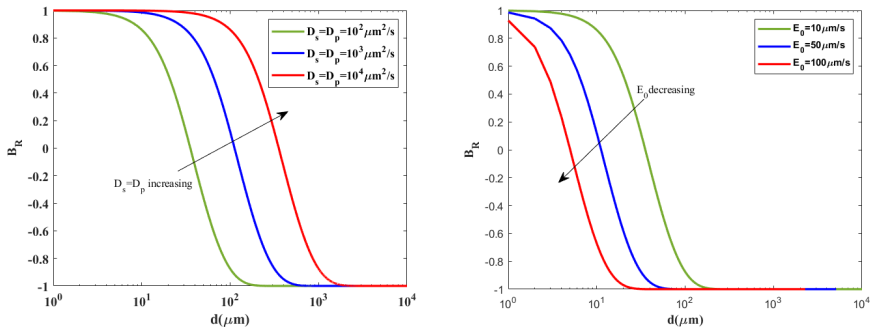

(a)

(b)

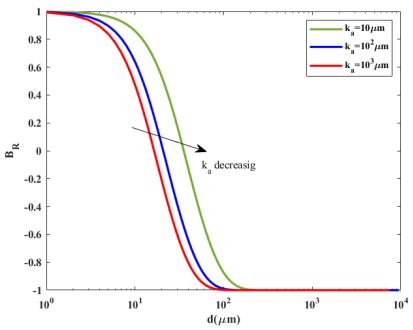

(c)

Figure 5. Resistance Eq.(3.8) vs enzyme membrane layer thickness $d\mu m$ with the parameters $D_s = D_p = 100\mu m^2/s$, $s_0 = 100$,$k_m = 10$, $k_2 = 100$, $E_0 = 1\mu m/s$, $k_a = 10$, $k_2 = 10$ and for different parameter values of (5(a)) diffusion coefficients of substrate and product D_s, D_p (5(b)) total enzyme concentrations E_0 (5(c)) kinetic parameter k_a.

where $B = 0$ and $A = \frac{1}{\cosh(m)}$ are obtained by applying boundary conditions Eq. (2.15) and Eq. (2.16) to the above equation. By changing the values of *A* and *B* in Eq. (B1), we obtain the solution of $S(\chi)$ as Eq. (3.1).
and by changing the governing equation Eq. (2.13) to Eq. (3.1), we obtain:

$$\frac{m^2\cosh(m\chi)}{\cosh m} = \frac{\left(\frac{\cosh(m\chi)}{\cosh(m)} + \left(\frac{\cosh(m\chi)}{\cosh(m)}\right)^2\right)}{1 + \beta\frac{\cosh(m\chi)}{\cosh(m)} + \gamma\left(\frac{\cosh(m\chi)}{\cosh(m)}\right)^2} \tag{B2}$$

By solving the above equation, we get:

$$m^2 = \frac{\phi_1^2(\cosh m + \alpha)\cosh m}{\cosh^2 m + \beta\cosh m + \gamma} \tag{B3}$$

Let apply the boundary condition Eq. (2.15) in Eq.(3.1),we get:

$$S(0) = \frac{1}{\cosh(m)} \tag{B4}$$

Substituting the S(χ) and S(0) in the equation Eq.(.9), the concentration of product equation P(χ) Eq.(3.3) as obtained as the dimensionless current equation Eq.(3.4).

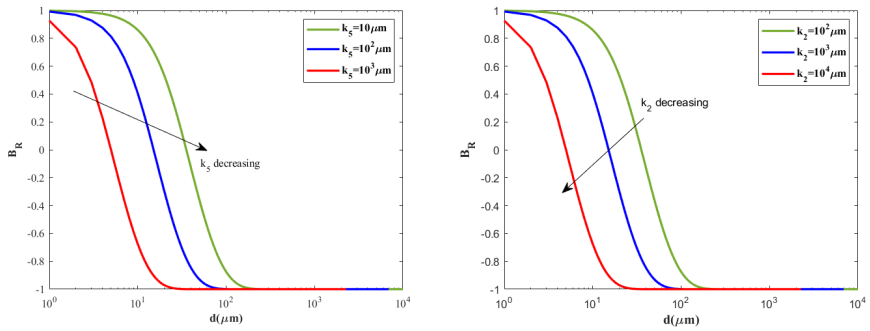

(a) (b)

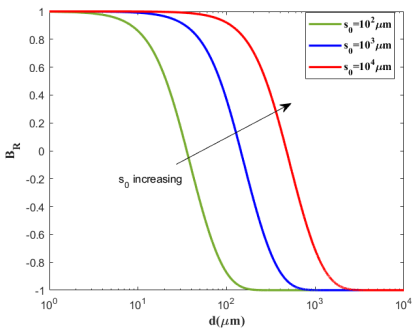

(c)

Figure 6. Resistance Eq.(3.8) vs enzyme membrane layer thickness $d\mu m$ with the parameters $D_s = D_p = 100\mu m^2/s$, $s_0 = 100$, $k_m = 10$, $k_2 = 100$, $E_0 = 1\mu m/s$, $k_a = 10$, $k_5 = 10$ and for different parameter values of (6(a)) kinetic parameter k_5 (6(b)) kinetic parameter k_2 (6(c)) bulk substrate concentration s_0.

Appendix C: Nomeclature

Symbol	name of symbol	Unit
s	Substrate's Concentration	μM
p	Product's Concentration	μM
s_0	Substrate's Concentration at $x = d$	μM
k_m	Constant of Michaelis-menten	μM
k_a, k_2, k_5	Constants of reaction rate	μM
E_0	Concentration of all Enzymes	$\mu M/s$
d	Enzyme layer thickness	μm
F	Faraday's constant	C/mol
D_s	The substrate's diffusion coefficient	$\mu m^2/s$
D_p	The product's diffusion coefficient	$\mu m^2/s$
Ψ	Current density	$\mu A/cm^2$
x	Distance	cm
n_e	Number of electrons take part in reaction	None
S	Concentration of dimensionless substrate	None
P	Concentration of dimensionless product	None
χ	Distance without dimensions	None
ϕ_1^2	Substrate's diffusion parameter	None
ϕ_2^2	Product's diffusion parameter	None
α	Parameter of saturation	None
β	Parameter of saturation	None
γ	Parameter of saturation	None
B_S	Biosensor's Sensitivity	None
B_R	Biosensor's Resistance	None

References

[1] J. Kulys and R. Baronas *Modelling of amperometric biosensors in the case of substrate inhibition*, Sensors, **6**, 1513–1522, (2006).

[2] R. Baronas, F. Ivanauskas, J. Kulys and M. Sapagovas, *Modelling of amperometric biosensors with rough surface of the enzyme membrane*, J. Math Chem., **34**, 227–242, (2003).

[3] D. Šimelevičius, and R. Baronas, *Computational modelling of amperometric biosensors in the case of substrate and product inhibition*, J. Math. Chem., **47**, 430–445, (2010).

[4] M. E. G. Lyons, *Transport and kinetics in electrocatalytic thin film biosensors: bounded diffusion with non-Michaelis-Menten reaction kinetics*, J Solid State Electrochem., **24**, 2751–2761, (2020).

[5] R. Baronas, F. Ivanauskas and J. Kulys, *Mathematical modeling of biosensors*. Springer International Publishing (2021).

[6] D. Yu, B. Blankert, J. C. Vire and J. M. Kauffman, *Biosensors in drug discovery and drug analysis*, Anal. Lett., **38**, 1687–1701, (2005).

[7] P. Manimozhi, A. Subbiah and L. Rajendran,*Solution of steady-state substrate concentration in the action of biosensor response at mixed enzyme kinetics*, Sens. Actuators B: Chem., **147**, 290–297, (2010).

[8] R. Swaminathan, M. C. Devi, L. Rajendran and K. Venugopal, *Sensitivity and resistance of amperometric biosensors in substrate inhibition processes*, J. Electroanal. Chem., **895**, 115527, (2021).

[9] R. Agarwal, *An analytical study of non-newtonian visco-inelastic fluid flowbetween two stretchable rotating disks*, Palestine J. Math., **11**, 184–201, (2022).

[10] M. Mallikarjuna and R. Senthamarai,*An amperometric biosensor and its steady state current in the case of substrate and product inhibition: Taylors series method and Adomian decomposition method*, J. Electroanal. Chem., **946**, 117699 (2023).

[11] M. A. Rasheed and A. T. Balasim, *Blow-up results for a reaction-diffusion equation with a dirichlet boundary condition*, Palestine J. Math. **13**, 263–270, (2024).

[12] J. H. He, *Homotopy perturbation method: a new nonlinear analytical technique. Applied Mathematics and computation*, **135**, 73–79, (2003).

[13] B. Dhivyadharshini, R. Senthamarai, *Mathematical analysis of a non linear prey predator system: Analytical approach by HPM*, AIP Conf. Proc., **2516**, 250008, (2022).

[14] T. Roy and D. K. Maiti, *An optimal and modified homotopy perturbation method for strongly nonlinear differential equations*, Nonlinear Dyn., **111**, 15215–15231, (2023).

[15] J. H. He, Y. O. El-Dib and A. A. Mady, *Homotopy perturbation method for the fractal toda oscillator*, Fractal and Fract., **5**, 93, (2021).

[16] O. Gonzalez-Gaxiola, A. Biswas, M. Ekici and S. Khan, *Highly dispersive optical solitons with quadratic cubic law of refractive index by the variational iteration method*, J. Optic., **51**, 29–36, (2022).

[17] M. Sivakumar, M. Mallikarjuna and R. Senthamarai, *A kinetic non-steady-state analysis of immobilized enzyme systems without external mass transfer resistance*, Int. J. Anal. App., **22**, 31, (2024).

[18] G. Suganya and R. Senthamarai, *Approximate Analytical Expression of Diffusive Lotka-Volterra Prey-Predator Equations via Variational Iteration Method*, J. App. Nonlinear Dyn., **11**, 741–753, (2022).

[19] Y. Yang and S. Liao, *Comparison between homotopy analysis method and homotopy renormalization method in fluid mechanics*, Eur. J. Mechanics-B/Fluid., **97**, 187–198, (2023).

[20] P.K. Masjedi and P. M. Weaver, *Analytical solution for arbitrary large deflection of geometrically exact beams using the homotopy analysis method*, App. Math. Model., **103**, 516–542, (2022).

[21] U. Biswal, S. Chakraverty, B. K. Ojha and A. K. Hussein, *Numerical investigation on nanofluid flow between two inclined stretchable walls by Optimal Homotopy Analysis Method*, J. Comput. Sci., **63**, 101759, (2022).

[22] M. Sivakumar, R. Senthamarai, L. Rajendran and M. E. G. Lyons, *Reaction and Kinetic Studies of Immobilized Enzyme Systems: Part-I Without External Mass Transfer Resistance*, Int. J. Electrochem. Sci., **17**, 221159, (2022).

[23] M. Sivakumar, R. Senthamarai, L. Rajendran, and M. E. G. Lyons, *Reaction and Kinetics Studies of Immobilized Enzyme Systems: PartII With External Mass Transfer Resistance*, Int. J. Electrochem. Sci., **17**, 221031, (2022).

[24] J.H. He, *A short review on analytical methods for a fully fourth-order nonlinear integral boundary value problem with fractal derivatives*, Int. J. Numer. Method. Heat and Fluid Flow., **30**, 4933–4943, (2020).

[25] S. Muthukaruppan, R. Senthamarai and L. Rajendran, *Modelling of immobilized glucoamylase kinetics by flow calorimetry*, Int. J. Electrochem. Sci., **7**, 9122–9137, (2012).

[26] M. Kumar and Umesh, *Recent development of Adomian decomposition method for ordinary and partial differential equations*, Int. J. Appl. Comput. Math., **8**, 81, (2022).

[27] M. Mallikarjuna and R. Senthamarai, *Mathematical analysis of batch reactor performance for the enzymatic synthesis of cephalexin: Laplace Homotopy perturbation method and Adomian decomposition method*, Partial. Diff. Equ. Appl. Math., **11**, 100806, (2024).

[28] J. Saelao and N. Yokchoo, *The solution of Klein Gordon equation by using modified Adomian decomposition method*, Math. Comput. Simul., **171**, 94–102, (2020).

[29] M. L. C. Mary, R. Saravanakumar, D. Lakshmanaraj, L. Rajendran and M. E. G. Lyons, *Mathematical modelling of unsteady flow of gas in a semi-infinite porous medium*, Int. J. Electrochem. Sci., **17**, 220619, (2022).

[30] K. M. Dharmalingam and M. Veeramuni, *Akbari-Ganji's Method (AGM) for solving non-linear reaction-Diffusion equation in the electroactive polymer film*, J. Electroanal. Chem., **844**, 1–5, (2019).

[31] M. E. G. Lyons, *Transport and kinetics in electrocatalytic thin film biosensors: bounded diffusion with non-Michaelis-Menten reaction kinetics*, J. Solid State Electrochem., **24**, 2751–2761, (2020).

[32] M. F. Najafabadi, H. TalebiRostami, K. Hosseinzadeh and D. D. Ganji, *Investigation of nanofluid flow in a vertical channel considering polynomial boundary conditions by Akbari-Ganji's method*, Theor. Appl. Mech. Lett., **12**, 100356, (2022).

Author information

K. Jegan, Department of Mathematics, College of Engineering and Technology, SRM Institute of Science and Technology, Kattankulathur-603203, India.
E-mail: jk6631@srmist.edu.in

M. Mallikarjuna, Department of Mathematics, College of Engineering and Technology, SRM Institute of Science and Technology, Kattankulathur-603203, India.
E-mail: mm0965@srmist.edu.in

R. Senthamarai, Department of Mathematics, College of Engineering and Technology, SRM Institute of Science and Technology, Kattankulathur-603203, India.
E-mail: senthamr@srmist.edu.in